INTER-NOISE 2018
Impact of Noise Control Engineering
26-29 AUGUST
CHICAGO, ILLINOIS

A low-rank iteration scheme for multi-frequency acoustic problems

Suhaib K. Baydoun[a], Lei Li, Steffen Marburg
Chair of Vibroacoustics of Vehicles and Machines
Department of Mechanical Engineering
Technical University of Munich
Boltzmannstraße 15, 85748 Garching, Germany

Matthias Voigt
Institut für Mathematik
Technische Universität Berlin
Straße des 17. Juni 136, 10623 Berlin, Germany

ABSTRACT

The boundary element method for the discretization of the Kirchhoff-Helmholtz integral equation is a popular numerical tool for solving linear time-harmonic acoustic problems. However, the implicit frequency dependence of the boundary element matrices necessitates an efficient treatment for problems requiring solutions in a frequency range. While several approaches based on approximations of the Green's function, the matrix, or even the solution itself exist in the literature, this paper presents an alternative method that provides a simultaneous solution over a frequency range within a single iterative scheme. A frequency approximation of the boundary element system in conjunction with a low-rank approximation of the solution enables efficient matrix vector multiplications. The algorithm can be incorporated into iterative solvers, such as BiCGstab in order to obtain the frequency range solution.

The proposed scheme is applied to an acoustic interior problem subject to different boundary conditions. The influence of both the approximation order and the accuracy of the low-rank truncations on the convergence behavior of the solution are studied. The results verify the effectiveness of the proposed iterative scheme. It opens up possibilities for the efficient evaluation of structural-acoustic interactions and associated phenomena in the future.

1 INTRODUCTION

The boundary element method (BEM) is widely used for solving linear time-harmonic acoustic problems arising in many technical and scientific applications [20]. Boundary element discretizations are restricted to the surface of the wave-carrying fluid domain, and hence, involve fewer degrees of freedom than corresponding discretizations obtained by the finite element method

[a] Corresponding author. Email: suhaib.baydoun@tum.de

(FEM). Moreover, the implicit satisfaction of the far field radiation condition is particularly advantageous for exterior problems compared to the FEM.

However, one of the major shortcomings of the BEM is the frequency dependence of the system matrix and right-hand side. Therefore, the numerical integration for setting up the fully populated matrices and the subsequent solution of the arising systems of equations need to be performed for each individual frequency of interest. In consequence, the computational effort for acoustic problems subjected to rapidly varying responses is considerably driven by the number of frequency steps, in particular if the solution is performed independently for each frequency.

A large number of methods for an efficient boundary element analysis over frequency ranges have been published in the last decades. The first approaches involve frequency interpolations of the boundary element matrices based on few matrices, which are computed at sample frequencies [3, 9]. Shortly thereafter, the interpolation of the Green's function used in the boundary integral equation was suggested, limiting the integration to a single frequency [19]. While these methods only address the computational effort associated with the set-up of the boundary element matrices, Raveendra proposed an iterative solution scheme, which uses the factored form of the matrices at the sample frequencies [15].

Instead of approximating the system matrix, Coyette employed a Padé approximation to calculate the frequency response from a single boundary element solution [5]. Padé approximations have also been used in the context of transfer matrices for an efficient multi-frequency calculation of the radiated sound power [1, 17]. Modal contributions to radiated sound power have been determined by solving the polynomial eigenvalue problem of coupled structural-acoustic interactions [14].

While acoustic problems involving a small number of degrees of freedom are amenable to direct solvers, most of today's engineering problems require iterative solution schemes such as Krylov subspace methods. In the course of solving a sequence of linear systems, the rate of convergence can be accelerated by retaining selected subspaces [8]. Krylov subspace recycling has been successfully applied to frequency range analyses with the BEM [7].

However, to the authors' knowledge, there is no indication of an iterative scheme allowing for a simultaneous solution for multiple frequencies in the literature. The approach in this paper is based on the work by Kressner [10] on parametric linear systems. A frequency approximation of the boundary element system in conjunction with a low-rank truncation of the solution enables efficient matrix vector multiplications. The algorithm is incorporated into the biconjugate gradient stabilized method (BiCGstab) in order to obtain the frequency range solution.

2 SIMULTANEOUS ITERATIVE SOLUTION OF MULTI-FREQUENCY BOUNDARY ELEMENT SYSTEMS

The acoustic BEM with a collocation discretization yields the frequency dependent linear system of equations

$$\mathbf{H}(k)\mathbf{p} = \mathbf{G}(k)\mathbf{v} = \mathbf{b}(k), \qquad \mathbf{H}(k), \mathbf{G}(k) \in \mathbb{C}^{n\times n}, \qquad \mathbf{p}, \mathbf{v}, \mathbf{b}(k) \in \mathbb{C}^{n\times 1}. \tag{1}$$

The vector $\mathbf{p}$ contains the unknown sound pressure values at the nodes. n denotes the number of nodes, which equals the number of unknowns. The boundary elements matrices $\mathbf{H}(k)$ and $\mathbf{G}(k)$ result from a collocation discretization of the Kirchhoff-Helmholtz integral equation, and they are fully populated, and neither Hermitian nor positive definite in general. They relate the particle velocity $\mathbf{v}$ to the sound pressure. Instead of storing $\mathbf{G}(k)$, the resulting right-hand side vector $\mathbf{b}(k)$

is usually assembled directly. All quantities are dependent on the wavenumber $k = 2\pi f/c$, where f and c denote the frequency and the speed of sound respectively.

In the context of a frequency range analysis, m linear systems need to be solved - one for each wavenumber of interest $k_1, k_2, \dots, k_m$. They can be arranged in a single system with a block diagonal matrix, i.e.

$$\begin{pmatrix} \mathbf{H}(k_1) & & \\ & \ddots & \\ & & \mathbf{H}(k_m) \end{pmatrix} \begin{pmatrix} \mathbf{p}_1 \\ \vdots \\ \mathbf{p}_\mathrm{m} \end{pmatrix} = \begin{pmatrix} \mathbf{b}(k_1) \\ \vdots \\ \mathbf{b}(k_m) \end{pmatrix}. \tag{2}$$

In order to simplify the matrix vector multiplication on the left-hand side of Eqn. (2), two approximations are introduced in what follows. The first one is a low-rank truncation of the solution. Therefore, the solutions $\mathbf{p}_1, \dots, \mathbf{p}_m$ are not stacked in a long vector as given in Eqn. (2), but arranged side-by-side in the matricization $\mathbf{P} \in \mathbb{C}^{n \times m}$, i.e. $\mathbf{P} = [\mathbf{p}_1, \dots, \mathbf{p}_m]$. Assuming a singular value decomposition and subsequent truncation, the solution matrix can be written as

$$\mathbf{P} \approx \mathbf{U}\mathbf{V}^*, \quad \mathbf{U} \in \mathbb{C}^{n \times r}, \quad \mathbf{V} \in \mathbb{C}^{m \times r}, \tag{3}$$

with the rank $r \ll n, m$. Secondly, an approximation of the frequency dependent system is introduced such that it has the form

$$\mathbf{H}(k) \approx \sum_{j=0}^{q} \mathbf{H}_j v_j(k), \tag{4}$$

with a small number of terms q, the frequency independent coefficient matrices $\mathbf{H}_j$, and the scalar valued, frequency dependent functions $v_j(\cdot)$. Combining the expressions (3) and (4), and defining the right-hand side matricization $\mathbf{B} = [\mathbf{b}_1, \dots, \mathbf{b}_m] \in \mathbb{C}^{n \times m}$, a linear operator $\boldsymbol{\mathcal{H}}: \mathbb{C}^{n \times m} \rightarrow \mathbb{C}^{n \times m}$ can be defined as

$$\boldsymbol{\mathcal{H}}(\mathbf{P}) = \sum_{j=0}^{q} (\mathbf{H}_j \mathbf{U})(\mathbf{V}^* \mathbf{D}_j), \quad \mathbf{D}_j = \mathrm{diag}\left(v_j(k_1), \dots, v_j(k_m)\right). \tag{5}$$

This operation can be viewed as an economic variant of the matrix vector multiplication on the left-hand side of Eqn. (2). The number of required operations is of $\mathcal{O}\left(qr(n^2 + m + mn)\right)$ compared to the subsequent matrix vector multiplications $\mathbf{H}(k_i)\mathbf{p}_i$ for m frequencies, which will result in $\mathcal{O}(mn^2)$. Details regarding the low-rank truncation and the approximation of the system matrix, as well as the incorporation of Eqn. (5) into an iterative solver are given in what follows.

2.1 Polynomial Approximation of the Boundary Element System Matrices

A polynomial approximation of the boundary element matrix is carried out in order to enable an economic application of the linear operator defined in Eqn. (5). Taylor approximations are the simplest type of polynomial approximations. However, they only provide a high accuracy in the vicinity of the Taylor point, and hence, the error is not evenly distributed across the frequency range [13]. Therefore, a q-th degree polynomial approximation of the form

$$\mathbf{H}(k) \approx \sum_{j=0}^{q} \mathbf{H}_j k^j = \mathbf{H}_0 + \mathbf{H}_1 k + \cdots + \mathbf{H}_q k^q \tag{6}$$

is used in this paper. The coefficient matrices $\mathbf{H}_j$ are obtained by sampling the frequency range of interest at $s \geq q+1$ sample frequencies and performing an entry-wise multiple linear regression using least squares [4]. The algorithm is implemented by the use of the MATLAB function `regress` available in MATLAB R2017b. The frequency samples are chosen as the Chebyshev nodes in order to minimize the effect of Runge's phenomenon [16]. For the wave number interval $k \in [k_{\min}, k_{\max}]$ they can be obtained from

$$k_j = 0.5(k_{\min} + k_{\max}) + 0.5(k_{\min} - k_{\max})\cos\frac{(2j-1)\pi}{2s}, \quad j \in [1, \ldots, s]. \tag{7}$$

The number of frequency samples and the polynomial orders that are required to meet certain error bounds are primarily dependent on the extent of the wave number interval, i.e. $k_{\max} - k_{\min}$. Moreover, for a given polynomial order, matrix entries associated with near field contributions are approximated more accurately than those related to far field contributions. However, rigorous studies on the relation between the approximation quality and the distance between source and field points are still missing.

2.2 Low-Rank Truncation of the Solution

A low-rank truncation of the solution matrix $\mathbf{P} \approx \mathbf{U}\mathbf{V}^*$ is required in order to efficiently apply the operator (5). Therefore, an economic singular value decomposition

$$\mathbf{P} = \widetilde{\mathbf{U}}\mathbf{\Sigma}\widetilde{\mathbf{V}}^* \tag{8}$$

is computed, where $\mathbf{\Sigma}$ contains the singular values $\sigma_1 \geq \cdots \geq \sigma_R$ on the diagonal with R denoting the rank of $\mathbf{P}$. Given the exponential decay of the singular values, which is proven for $\mathbf{P}$ and $\mathbf{B}$ since $\mathbf{H}(k)$ and $\mathbf{b}(k)$ are analytically frequency dependent [10], the truncation rank r is the smallest value such that

$$\sqrt{\sigma_{r+1}^2 + \cdots + \sigma_R^2} \leq \epsilon_{\text{svd}} \sqrt{\sigma_1^2 + \cdots + \sigma_r^2}. \tag{9}$$

The predefined relative error ϵ_{svd} controls the accuracy of the truncation, such that $\|\mathbf{P} - \mathbf{U}\mathbf{V}^{\mathrm{T}}\|_F \leq \epsilon_{\text{svd}} \|\mathbf{U}\mathbf{V}^{\mathrm{T}}\|_F$. $\mathbf{U}$ and $\mathbf{V}$ are then build up by using only the first r column vectors $\tilde{\mathbf{u}}$ and $\tilde{\mathbf{v}}$ of $\widetilde{\mathbf{U}}$ and $\widetilde{\mathbf{V}}$, i.e.

$$\mathbf{U} = [\tilde{\mathbf{u}}_1, \ldots, \tilde{\mathbf{u}}_r]\operatorname{diag}\left(\sqrt{\sigma_1}, \ldots, \sqrt{\sigma_r}\right), \quad \mathbf{V} = [\tilde{\mathbf{v}}_1, \ldots, \tilde{\mathbf{v}}_r]\operatorname{diag}\left(\sqrt{\sigma_1}, \ldots, \sqrt{\sigma_r}\right). \tag{10}$$

In this way, the truncation operator $\boldsymbol{\mathcal{T}}: \mathbb{C}^{n\times m} \to \mathbb{C}^{n\times m}, \mathbf{P} \mapsto \mathbf{U}\mathbf{V}^*$ can be defined, where $\mathbf{U}$ and $\mathbf{V}$ are obtained as in Eqn. (10).

2.3 The Biconjugate Gradient Stabilized Method for the Frequency Range Solution

BiCGstab [18] is a Krylov subspace method and particularly suited for the solution of non-symmetric linear systems of equations, as those arising from the acoustic BEM. However, the implementation used in this paper is non-standard in the sense that the iterate is a matrix instead of a vector. Moreover, a preconditioner $\boldsymbol{\mathcal{M}}: \mathbb{C}^{n\times m} \to \mathbb{C}^{n\times m}$ can be employed, which should be defined such that $\boldsymbol{\mathcal{M}}^{-1}$ can be economically applied to matrices in the low-rank format (3). The algorithm is summarized below. In there, inner products of two matrices $\langle \mathbf{X}, \mathbf{Y} \rangle$ need to be evaluated, which can be performed economically, if $\mathbf{X} = \mathbf{U}_x \mathbf{V}_x^*$ and $\mathbf{Y} = \mathbf{U}_y \mathbf{V}_y^*$ are available in the low-rank format as

$$\langle \mathbf{X}, \mathbf{Y} \rangle = \operatorname{trace}(\mathbf{X}^* \mathbf{Y}) = \operatorname{trace}\left(\left(\mathbf{V}_y^* \mathbf{V}_x \right) \left(\mathbf{U}_x^* \mathbf{U}_y \right) \right). \quad (11)$$

Algorithm 1 – Preconditioned BiCGstab for multi-frequency acoustic problems.

Input:	Linear operator $\boldsymbol{\mathcal{H}}: \mathbb{C}^{n\times m} \to \mathbb{C}^{n\times m}$ as given in Eqn. (5) Preconditioner $\boldsymbol{\mathcal{M}}: \mathbb{C}^{n\times m} \to \mathbb{C}^{n\times m}$ Truncation operator $\boldsymbol{\mathcal{T}}: \mathbb{C}^{n\times m} \to \mathbb{C}^{n\times m}$ as described in Sec. 2.2 Relative error for the low-rank approximation ϵ_{svd} Relative error for the residual ϵ_{tol} Right-hand side $\mathbf{B} \in \mathbb{C}^{n\times m}$	
Set:	$\boldsymbol{\mathcal{T}}(\mathbf{B}) \coloneqq \mathbf{B}$ Initial guess $\mathbf{P}_0 \coloneqq \mathbf{0}$, $\mathbf{R}_0 \coloneqq \mathbf{B}$ $\rho_0 \coloneqq \langle \mathbf{B}, \mathbf{R}_0 \rangle$ $\mathbf{Y}_0 \coloneqq \mathbf{R}_0$ $\widetilde{\mathbf{Y}}_0 \coloneqq \boldsymbol{\mathcal{M}}^{-1}(\mathbf{Y}_0)$, $\mathbf{W}_0 \coloneqq \boldsymbol{\mathcal{H}}(\widetilde{\mathbf{Y}}_0)$, $j \coloneqq 0$	 $\widetilde{\mathbf{Y}}_0 \coloneqq \boldsymbol{\mathcal{T}}(\widetilde{\mathbf{Y}}_0)$ $\mathbf{W}_0 \coloneqq \boldsymbol{\mathcal{T}}(\mathbf{W}_0)$
While	$\lVert \mathbf{R}_j \rVert_F / \lVert \mathbf{B} \rVert_F < \epsilon_{\mathrm{tol}}$ $\alpha_j \coloneqq \rho_j / \langle \mathbf{B}, \mathbf{W}_j \rangle$, $\mathbf{S}_j \coloneqq \mathbf{R}_j - \alpha_j \mathbf{W}_j$, $\tilde{\mathbf{S}}_j \coloneqq \boldsymbol{\mathcal{M}}^{-1}(\mathbf{S}_j)$, $\mathbf{T}_j \coloneqq \boldsymbol{\mathcal{H}}(\tilde{\mathbf{S}}_j)$, If $\lVert \mathbf{S}_j \rVert_F / \lVert \mathbf{B} \rVert_F < \epsilon_{\mathrm{tol}}$ $\mathbf{P} \coloneqq \mathbf{P}_j + \alpha_j \widetilde{\mathbf{Y}}_j$, return End if $\xi_j \coloneqq \langle \mathbf{T}_j, \mathbf{S}_j \rangle / \langle \mathbf{T}_j, \mathbf{T}_j \rangle$, $\mathbf{P}_{j+1} \coloneqq \mathbf{P}_j + \alpha_j \widetilde{\mathbf{Y}}_j + \xi_j \tilde{\mathbf{S}}_j$ $\mathbf{R}_{j+1} \coloneqq \mathbf{S}_j - \xi_j \mathbf{T}_j$, $\rho_{j+1} \coloneqq \langle \mathbf{B}, \mathbf{R}_{j+1} \rangle$ $\beta_j \coloneqq (\rho_{j+1} \alpha_j)/(\rho_j \xi_j)$, $\mathbf{Y}_{j+1} \coloneqq \mathbf{R}_{j+1} + \beta_j (\mathbf{Y}_j + \xi_j \mathbf{W}_j)$, $\widetilde{\mathbf{Y}}_{j+1} \coloneqq \boldsymbol{\mathcal{M}}^{-1}(\mathbf{Y}_{j+1})$,	 breakdown if $\langle \mathbf{B}, \mathbf{W}_j \rangle = 0$ $\mathbf{S}_j \coloneqq \boldsymbol{\mathcal{T}}(\mathbf{S}_j)$ $\tilde{\mathbf{S}}_j \coloneqq \boldsymbol{\mathcal{T}}(\tilde{\mathbf{S}}_j)$ $\mathbf{T}_j \coloneqq \boldsymbol{\mathcal{T}}(\mathbf{T}_j)$ $\mathbf{R}_{j+1} \coloneqq \boldsymbol{\mathcal{T}}(\mathbf{R}_{j+1})$ breakdown if $\rho_j \xi_j = 0$ $\mathbf{Y}_{j+1} \coloneqq \boldsymbol{\mathcal{T}}(\mathbf{Y}_{j+1})$ $\widetilde{\mathbf{Y}}_{j+1} \coloneqq \boldsymbol{\mathcal{T}}(\widetilde{\mathbf{Y}}_{j+1})$

$$\mathbf{W}_{j+1} := \mathcal{H}(\widetilde{\mathbf{Y}}_{j+1}), \qquad \mathbf{W}_{j+1} := \mathcal{T}(\mathbf{W}_{j+1})$$

$j := j + 1$

End while

Output: Sound pressure solution $\mathbf{P} \in \mathbb{C}^{n \times m}$ with $\|\mathcal{H}(\mathbf{P}) - \mathbf{B}\|_F / \|\mathbf{B}\|_F \leq \epsilon_{\text{tol}}$

Note that for the efficiency of the method, it is crucial that the right-hand side **B** and the solution matrix **P** both admit a low-rank factorization. Otherwise, the intermediate matrices computed in Algorithm 1 are not of low numerical rank and the inner products could not be computed efficiently as in (11). However, in our application, this low-rank structure is usually present.

3 NUMERICAL EXAMPLE

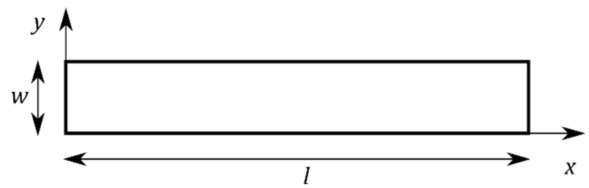

Figure 1 – Geometry of the two-dimensional duct.

The proposed scheme is applied to an acoustic interior problem in order to provide a proof of concept. A plane sound wave in a closed, rigid two-dimensional duct of length $l = 3.4$ m and width $w = 0.2$ m is considered, as shown in Fig. 1. It is filled entirely with air with a density of $\rho = 1.3\ \text{kg/m}^3$, and the speed of sound is $c = 340\ \text{m/s}$. A sound wave is generated due to a harmonic excitation by a particle velocity of $v_0 = 1$ mm/s at $x = 0$. The example is studied in the frequency range from 421 to 520 Hz in steps of $\Delta f = 1$ Hz, i.e. $m = 100$. Two different boundary conditions are considered. First, an admittance boundary condition with $Y(l) = 1/\rho c$ used, which results in a travelling wave that is fully absorbed at the end $x = l$ of the duct. Secondly, acoustically rigid boundary conditions $Y(l) = 0$ are used, leading to a full reflection of the wave, and hence, standing waves emerge at the resonance frequencies of 450 and 500 Hz. The three-dimensional equivalent of this model is defined as a benchmark problem of computational acoustics [6] and rigorous studies on associated numerical errors exist [2, 11].

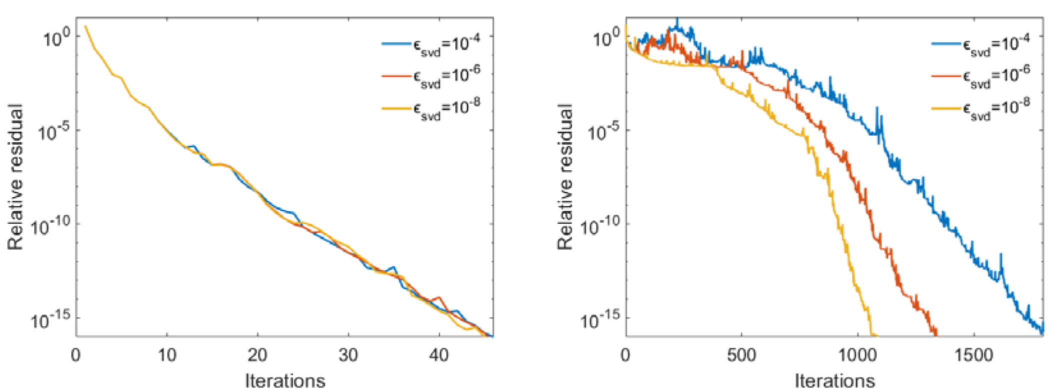

Figure 2 – Convergence of the BiCGstab for $q = 6$ and different tolerances for the low-rank truncation. Results for the fully absorbing (left) and for the acoustically rigid condition (right).

The mesh consists of 32 one-dimensional boundary elements with quadratic Lagrangian pressure approximation, of which 15 elements are employed for both edges parallel to the direction of wave propagation, respectively. This corresponds to $n = 64$ degrees of freedom, and hence,

$\mathbf{H}(k) \in \mathbb{C}^{64\times 64}$. The ranks of $\mathbf{P}$ and $\mathbf{B}$ after computing the singular value decompositions and performing truncations with different accuracies ϵ_{svd} are given in Table 1. The ranks are considerably smaller than n and m, and hence, the products in Algorithm 1 can be efficiently computed by making use of the low-rank format. However, note that the ranks of the intermediate matrices could temporarily increase in the course of the iterations.

Polynomial approximations of orders $q = 3, \ldots, 6$ are calculated, whereas the sample frequencies are chosen according to Eqn. (7). For the sake of efficiency, the right-hand side vectors are also only computed at those sample frequencies and interpolated across the frequency range. No preconditioning is used, i.e. $\boldsymbol{\mathcal{M}} = \mathbf{I}$.

Table 1 – Ranks of conventionally calculated solutions matrices **P** and right-hand sides **B** after low-rank truncations with different accuracies ϵ_{svd}

	$\epsilon_{\mathrm{svd}} = 10^{-4}$	$\epsilon_{\mathrm{svd}} = 10^{-6}$	$\epsilon_{\mathrm{svd}} = 10^{-8}$
Rank of **P** for case I	6	8	10
Rank of **P** for case II	7	9	11
Rank of **B**	5	7	7

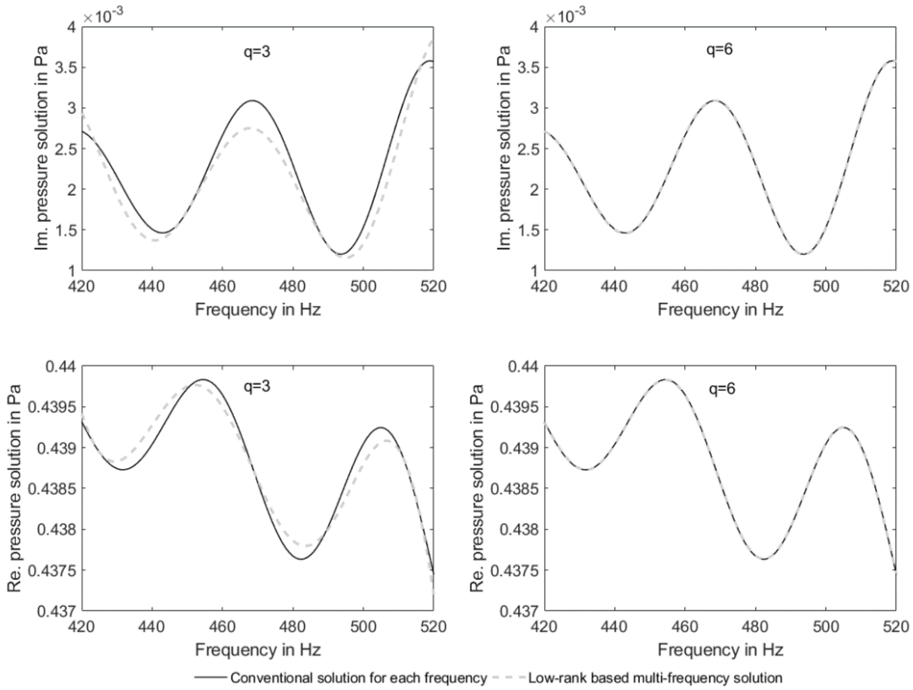

Figure 3 – Imaginary and real parts of the sound pressure solution in the fully absorbing case at the corner $(x, y) = (0,0)$ of the duct. Comparison of the multi-frequency solutions with polynomial approximations of order $q = 3$ and $q = 6$ and the conventional, frequency-wise solution.

The convergence of the relative residuals $\|\mathbf{R}\|_F / \|\mathbf{B}\|_F$ for both, the fully absorbing case (I) and the acoustically rigid case (II), are shown in Fig. 2. In case (I), different accuracies of the low-rank truncations ϵ_{svd} do not have a significant influence on the convergence, while in case (II), higher accuracies are associated with faster convergence. Moreover, the truncations do not cause an early stagnation of the method in both conditions. While in the absorbing case (I), convergence is reached rather quickly, the convergence rate in the rigid case (II) is much slower due to the non-smoothness of the sound pressure solution at the resonance frequencies.

Figure 3 shows the real and imaginary parts of the sound pressure solutions in the absorbing case (I) at the corner node $(x, y) = (0,0)$. The results are obtained by means of the proposed iterative scheme with polynomial approximations of order $q = 3$ and $q = 6$. The comparison to the conventionally (i.e. frequency-wise) obtained results indicates a good agreement. Similar graphs are displayed for the rigid case (II) in Fig. 4. Despite the non-smoothness associated with the resonance peaks, the multi-frequency solutions accord well with the reference solutions. Similarly good agreements are also achieved for all other positions in the duct.

Regarding the overall accuracy of the multi-frequency solutions, the approximation of the system matrix and the truncation of the solution introduce further numerical errors in addition to the common discretization error. While the error associated with the truncation can be controlled by the predefined tolerance ϵ_{svd}, the quality of the polynomial matrix interpolation cannot be predicted a-priori. Further studies are required to gain confidence in this regard.

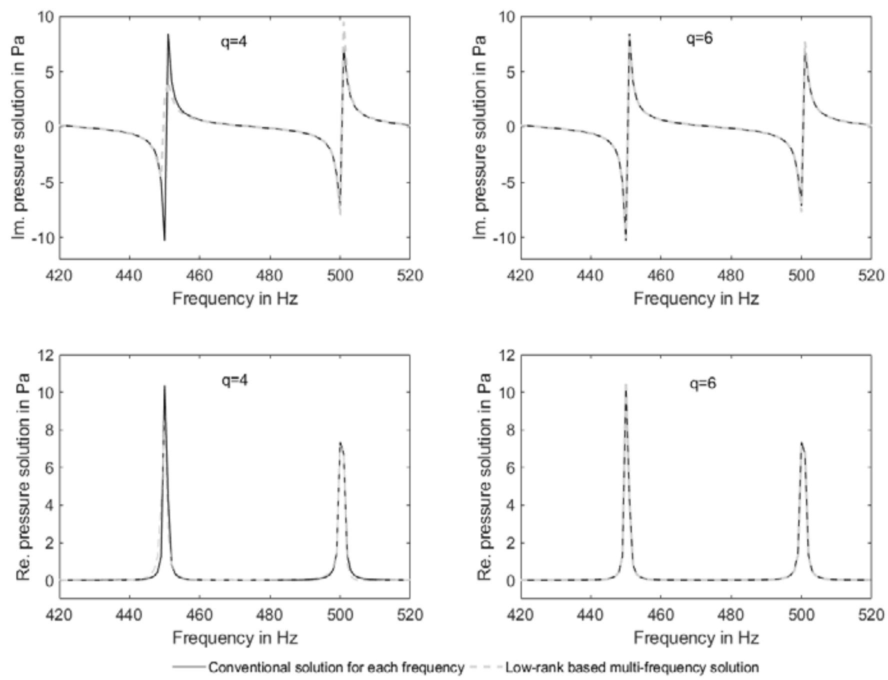

Figure 4 - Imaginary and real parts of the sound pressure solution in the acoustically rigid case at the corner $(x, y) = (0,0)$ of the duct. Comparison of the multi-frequency solutions with polynomial approximations of order $q = 4$ and $q = 6$ and the conventional, frequency-wise solution.

4 CONCLUSIONS AND FUTURE WORK

A polynomial frequency approximation of the boundary element system in conjunction with low-rank approximations of the solution have been used to enable efficient matrix vector multiplications in the course of solving multi-frequency acoustic problems with BiCGstab. The process has been applied to an interior problem subject to fully absorbing and rigid boundary conditions. Both scenarios have shown convergence, though a relatively large number of iterations was required for the rigid case exhibiting a resonant behavior. On the other hand, in the absorbing case, convergence has been reached much faster due to the smoothness of the solution resulting in a much shorter computational time. A conventional approach with an individual solution process for each frequency obviously requires similar amounts of computational effort in both cases. Therefore, the presented scheme is advantageous in the sense that the computational effort is adjusted automatically, and consequently, less a-priori knowledge of the solution complexity is needed. In cases, where the sound pressure exhibits large variations across the frequency range of interest, smaller partitions of the solution matrix are truncated.

The main purpose of this paper is to present the multi-frequency scheme and to provide a preliminary verification. Therefore, only problems with a small number of degrees of freedom have been descriptively studied in order to provide a proof of concept. Of course, larger problems need to be considered in order to actually benefit from an iterative scheme and also in view of useful comparisons with existent multi-frequency strategies. On the other hand, the size of the problem is limited due to the need to store several fully populated matrices. An incorporation of the hierarchical format could address this issue.

Apart from that, different parts of the algorithm should be improved in the future. First and foremost, an efficient preconditioning needs to be found that works for the whole frequency range. In addition, different frequency approximations such as the discrete empirical interpolation method are possible [12]. More efficient strategies for the low-rank truncation and for the sampling are also eligible. Further, the procedure could be incorporated into other iterative schemes such as GMRes. Finally, the multi-frequency scheme could also be applied to structural-acoustic interactions and associated phenomena such as frequency-dependent radiation damping.

5 ACKNOWLEDGEMENTS

This work has been conducted with the support of the German Research Foundation (DFG) in the context of the priority program 1897 “Calm, Smooth and Smart - Novel Approaches for Influencing Vibrations by Means of Deliberately Introduced Dissipation”.

6 REFERENCES

[1] J. Baumgart, S. Marburg, and S. Schneider, “Efficient sound power computation of open structures with infinite/finite elements and by means of the Padé-via-Lanczos algorithm”, *Journal of Computational Acoustics*, **15**(4), 557-577 (2007).

[2] S. Baydoun and S. Marburg, “Quantification of numerical damping in the acoustic boundary element method for two-dimensional duct problems”, *Journal of Theoretical and Computational Acoustics,* (2018). (Accepted for publication.)

[3] G. W. Benthien and H. A. Schenk, “Structural-acoustic coupling”, in *Boundary Element Methods in Acoustics*, edited by R. D. Ciskowski and C. A. Brebbia, Computational Mechanics Publications, Elsevier Applied Science (1991).

[4] S. Chatterjee and A. S. Hadi, “Influential observations, high leverage points, and outliners in linear regression”, *Statistical Science*, **1**(3), 379-416 (1986).

[5] J.-P. Coyette, C. Lecomte, and J.-L. Migeot, “Calculation of vibro-acoustic frequency response functions using a single frequency boundary element solution and a Padé expansion”, *Acta Acustica United with Acustica*, **85**(3), 371-377 (1999).

[6] M. Hornikx, M. Kaltenbacher, and S. Marburg, “A platform for benchmark cases in computational acoustics”, *Acta Acustica United with Acustica*, **101**(4), 811-820 (2015).

[7] S. Keuchel, J. Bierman, and O. von Estorff, "A combination of the fast multipole boundary element method and Krylov subspace recycling solvers", *Engineering Analysis with Boundary Elements*, **65**, 136-146 (2016).

[8] M. E. Kilmer and E. de Sturler, "Recycling subspace information for diffuse optical tomography", *SIAM Journal on Scientific Computing*, **27**(6), 2140-2166 (2006).

[9] S. M. Kirkup and D. J. Henwood, "Methods for speeding up the boundary element solutions of acoustic radiation problems", *Journal of Vibration and Acoustics,* **114**(3), 374-380 (1992).

[10] D. Kressner and C. Tobler, "Low-rank tensor Krylov subspace methods for parametrized linear systems", *SIAM Journal on Matrix Analysis and Applications*, **32**(4), 1288-1316 (2011).

[11] S. Marburg, "A pollution effect in the boundary element method for acoustic problems", *Journal of Computational Acoustics*, **26** (2018). Available online at: https://doi.org/10.1142/S0218396X18500182

[12] F. Negri, A. Manzoni, and D. Amsallem, "Efficient model reduction of parametrized systems by matrix discrete empirical interpolation", *Journal of Computational Physics*, **303**, 431-454 (2015).

[13] H. Peters, N. Kessissoglou, and S. Marburg, "Modal decomposition of exterior acoustic-structure interaction", *Journal of Acoustical Society of America*, **133**(5), 2668-2677 (2013).

[14] H. Peters, N. Kessissoglou, and S. Marburg, "Modal decomposition of exterior acoustic-structure interaction problems with model order reduction", *Journal of Acoustical Society of America*, **135**(5), 2706-2717 (2014).

[15] S. T. Raveendra, "An efficient indirect boundary element technique for multi-frequency acoustic analysis", *International Journal for Numerical Methods in Engineering*, **44**(1), 59-76 (1999).

[16] C. Runge, "Über empirische Funktionen und die Interpolation zwischen äquidistanten Ordinaten", *Zeitschrift für Mathematik und Physik*, **46**, 224-243 (1901).

[17] J. P. Tuck–Lee, P. M. Pinsky, and H.–L. Liew, "Multifrequency analysis using matrix Padé–via–Lanczos", in *Computational Acoustics of Noise Propagation in Fluids. Finite and Boundary Element Methods*, edited by S. Marburg and B. Nolte, Springer, Berlin, Heidelberg (2008).

[18] H. A. van der Horst, "Bi-CGSTAB: A fast and smoothly converging variant of Bi-CG for the solution of nonsymmetric linear systems", *SIAM Journal on Scientific and Statistical Computing* **13**(2), 613-644 (1992).

[19] T. W. Wu, W. L. Li, and A. F. Seybert, "An efficient boundary element algorithm for multi-frequency acoustical analysis", *Journal of Acoustical Society of America*, **94**(1), 447-542 (1993).

[20] T. W. Wu (ed.), *Boundary Element Acoustics: Fundamentals and Computer Codes,* WIT Press, Southampton (2000).